

multiplicity to give rise to a plateau around the shower axis. With the same value of ϵ but with primary energies 10^{14} ev and 4×10^{14} ev we get particle densities which are respectively half and twice the observed value and the angular spreads, too, are in error. Thus the value of the primary energy which can generate showers of minimum energy seem to be fixed quite sensitively. If we now alter the value of ϵ , keeping the primary energy fixed at 2×10^{14} ev, the results are not so sensitively affected. But the values for $\epsilon=0.15$ and $\epsilon=0.01$ are in error since in the former case the angular spread is nearly twice and in the latter case half of what is required by experiment and particle densities around the shower axis also be in error by magnitudes of the same order. The value of $\epsilon=0.05$, chosen as giving best agreement with experimental results corresponds to the field mass being equal to $\frac{1}{3}$ the mass of the π mesons.

CONCLUSION

It is shown that on the basis of Fermi's model of meson production it is not possible to generate showers

of the minimum size which contain 500 particles per square meter around the shower axis and no multiple peaks separated by distances more than a meter. On the other hand, Bhabha's modification to the phenomenological models predicts a more concentrated angular distribution which seems to be in accord with the requirements for the showers of minimum size. A comparison between the theoretical calculations based on this theory and the experimental data leads to a value of ϵ , the ratio of field mass to proper mass, which appears to be reasonable. These satisfactory results may be accidental but they form one more bit of evidence for the importance of the structure of nucleons and mesons in all phenomena concerning the interactions of nucleons among themselves or the interactions between nucleons and mesons.

ACKNOWLEDGMENTS

I wish to express my thanks to Professor H. J. Bhabha for his kind interest in this problem.

Albedo of Cosmic Rays in the Earth's Dipole and Quadrupole Magnetic Field*

RUTH GALL, *Instituto Nacional de la Investigación Científica, Instituto de Geofísica, México, D. F., México*

AND

JAIME LIFSHITZ, *Instituto Nacional de la Investigación Científica, México, D. F., México*

(Received December 6, 1955)

Albedo trajectories for protons of 0.5, 1.0, 1.5, and 2.0 Bev in the earth's dipole and quadrupole magnetic field were computed. The zenithal, azimuthal, latitude, and magnetic rigidity effects were studied. The quadrupole induces an asymmetry which seems only to be important near the geomagnetic equator. Shadow cones were obtained for one point of incidence.

INTRODUCTION

THE present work on albedo consisted in calculating 412 trajectories of secondary protons in the earth's magnetic field. The energies chosen for the particles were 0.5, 1.0, 1.5, and 2.0 Bev. (The same trajectories are followed by alpha particles of energies shown in Table I.)

TABLE I. The relations between the values of the constant C , the magnetic rigidity R , and the energies E_p , E_α of protons and alpha particles.

| C | $10^{-9}R$ (volts) | E_p (Bev) | E_α (Bev) |
|---------|--------------------|-------------|------------------|
| 13.5682 | 1.091 | 0.50 | 0.59 |
| 8.7206 | 1.697 | 1.00 | 1.31 |
| 6.5720 | 2.252 | 1.50 | 2.12 |
| 5.3118 | 2.786 | 2.00 | 2.97 |

* Presented at the Fifth International Congress of Cosmic Rays, September, 1955 in Guanajuato, México.

The model used for the magnetic field is that of Schmidt and Chargoy.^{1,2} It consists of a dipole and a quadrupole, both eccentric, the axes of which form an orthogonal system. The origin of this system resides at the point $(-344, 150, 96)$ in km, given in geographic coordinates.³ The magnitude of the quadrupole field,

TABLE II. The geomagnetic coordinates of the seven incidence points on the earth's surface; the ratio of the quadrupole field (H_c) to the dipole field (H_d); the number of trajectories computed (N).

| Point | 1 | 2 | 3 | 4 | 5 | 6 | 7 |
|-------------|--------|------|------|------|------|------|------|
| λ | 30°N | 75°N | 75°N | 75°N | 60°N | 0° | 0° |
| ϕ | 22.5°E | 0° | 90°E | 45°E | 45°E | 45°E | 0° |
| $H_c/H_d\%$ | 8.4 | 1.5 | 1.5 | 0.9 | 3.4 | 15.9 | 10.6 |
| N | 244 | 16 | 16 | 16 | 16 | 52 | 52 |

¹ S. Chapman and J. Bartels, *Geomagnetism, II* (Clarendon Press, Oxford, 1940), p. 651.

² A. Chargoy, *Revista Mexicana de Física*, 2, 1 (1953).

³ Based on the map of the geomagnetic field of 1945.

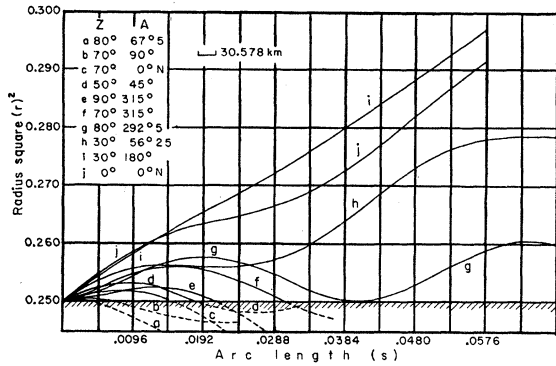


FIG. 1. The orbits of secondary protons of energy 0.5 BeV in the earth's dipole and quadrupole magnetic field. Point of incidence: $\lambda=30^\circ N$, $\varphi=22.5^\circ E$. The inset table indicates the zenith and azimuth angles of incidence.

relative to that of the dipole, varies with the geomagnetic longitude and latitude and is maximum at the geomagnetic equator, where its highest value is 16%.

Choosing a velocity equal to 1 and taking the earth's radius to be 0.5, the differential equation of motion becomes

$$\frac{d^2 \mathbf{r}}{dt^2} = C \frac{d\mathbf{r}}{dt} \times \left[\nabla \left(\frac{z}{r^3} \right) + \alpha \nabla \left(\frac{xy}{r^5} \right) \right]. \quad (1)$$

C is inversely proportional to the magnetic rigidity of the particle: $C = -m_1 a q / 4 p c$; where a is the earth's radius, equal to 6.371×10^8 cm, q is the charge of the proton in esu, c the velocity of light, p the relativistic momentum of the particle. Also, $\alpha = 3m_2 / 4m_1$, a con-

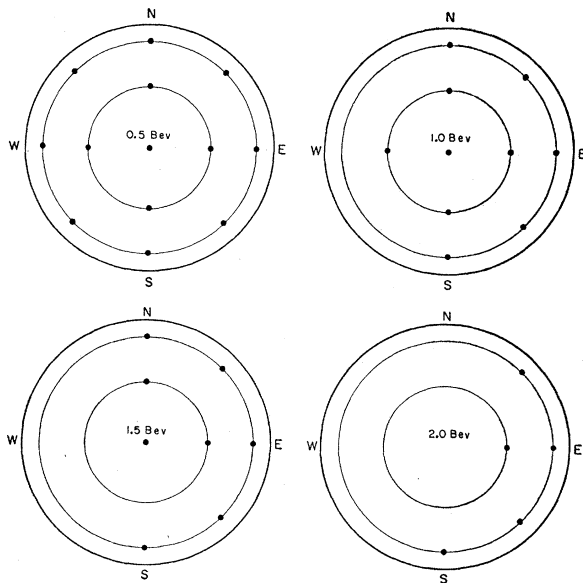


FIG. 2. Orbits of secondary protons in the earth's shadow. Point of incidence: $\lambda=0^\circ$, $\varphi=0^\circ$. Projection of the unit sphere on the horizontal plane. The solid points represent the directions of incidence in the earth's shadow, for energies of 0.5, 1.0, 1.5, 2.0 BeV.

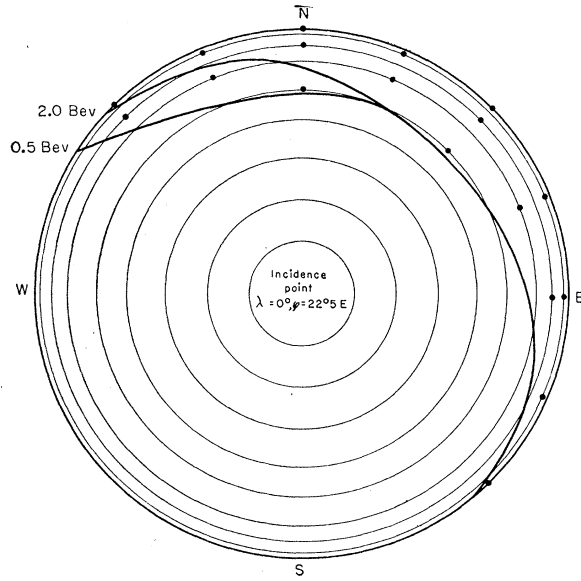


FIG. 3. Simple shadow cones for secondary protons of 0.5 and 2.0 BeV. The circle represents the projection of the unit sphere on the horizontal plane. The solid points represent the directions in the earth's shadow.

stant; here $m_1 = M_d / a^3 = 0.3097$ gauss, $m_2 = M_c / a^4 = 0.0219$ gauss, and M_d , M_c are the dipole and quadrupole moments, respectively.

No integral except that of conservation of velocity was found; therefore a unit of length analogous to that of Störmer could not be introduced.

Seven points of incidence on the earth's surface were chosen. (See Table II.) Point 1 was chosen to have medium latitude and longitude. Points 2, 3, 4, 5, latitudes larger than the knee for 1950 and points 6 and 7 at the geomagnetic equator at longitudes of maximum and minimum magnitude of the quadrupole field.

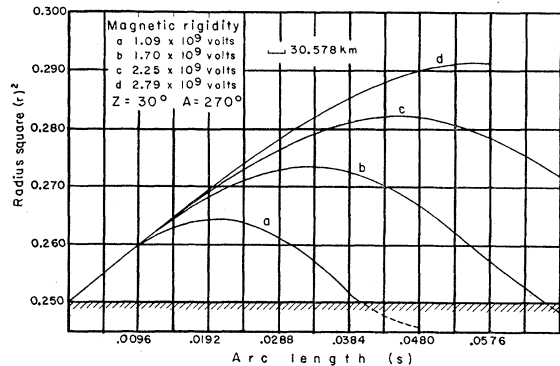


FIG. 4. Effect of the magnetic rigidity on the albedo trajectories. Point of incidence: $\lambda=0^\circ$, $\varphi=0^\circ$. The table contains the magnetic rigidities of the protons and the direction of incidence. The plot shows four trajectories followed by four particles of different energies incident on the same point, in the same direction.

⁴ W. E. Milne, *Numerical Calculus* (Princeton University Press, Princeton, 1949), p. 135.

The method suggested by Milne⁴ was used in the numerical integration. The integration formulas are: "Predictor":

$$f_n = f_{n-4} + (4h/3)(2f'_{n-1} - f'_{n-2} + 2f'_{n-3}), \quad (2)$$

"Corrector":

$$f_n = f_{n-2} + (h/3)(f'_{n-1} + 4f'_{n-2} + f'_{n-3}). \quad (3)$$

The interval between equally spaced points is $h=0.0024$ ($=30.578$ km). The maximum length traveled along the trajectory is 860 km. The position of the particle as calculated is precise to the third significant figure, as with the interval chosen the accumulated error over the 28 points of travel does not affect the third decimal. With the interval chosen for each point of the trajectory, the field and the position had to be calculated only once. The velocity was calculated first by the "predictor" [Eq. (2)], then by the "corrector" [Eq. (3)]. From these two approximations to the velocity, two values of the acceleration were obtained by Eq. (1). The calculations were performed with the IBM Punch Card Calculating Machine, Model 602 A. Several other auxiliary IBM machines were used.

GRAPHIC REPRESENTATION OF RESULTS

The results are shown graphically in Figs. 1-8. The graphic representation is also valid for alpha particles of the energies appearing in Table I. It should be pointed out that in Figs. 1, 4, 5(a), 5(b), 6(a), 6(b), 6(c), 7(a), and 7(b), the curves do not represent projections of

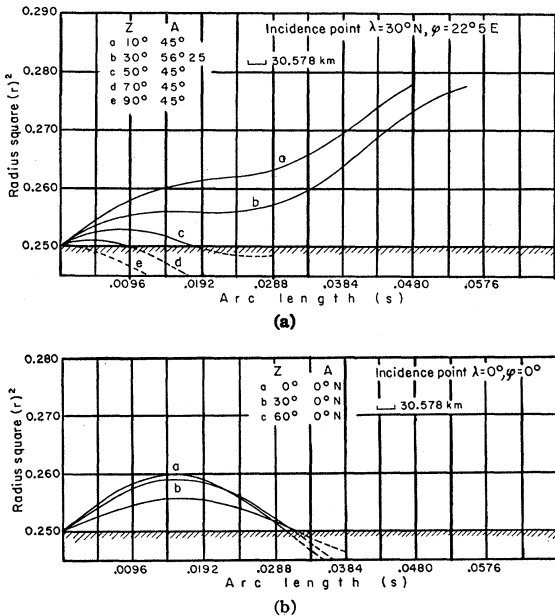


FIG. 5. The effect of zenith angle on albedo. Trajectories of protons of 0.5 Bev. The inset tables indicate the values of the azimuth angle and the variable zenith angles. Two different points of incidence are considered. The comparison of the two figures shows the influence of the latitude on the zenith angle effect.

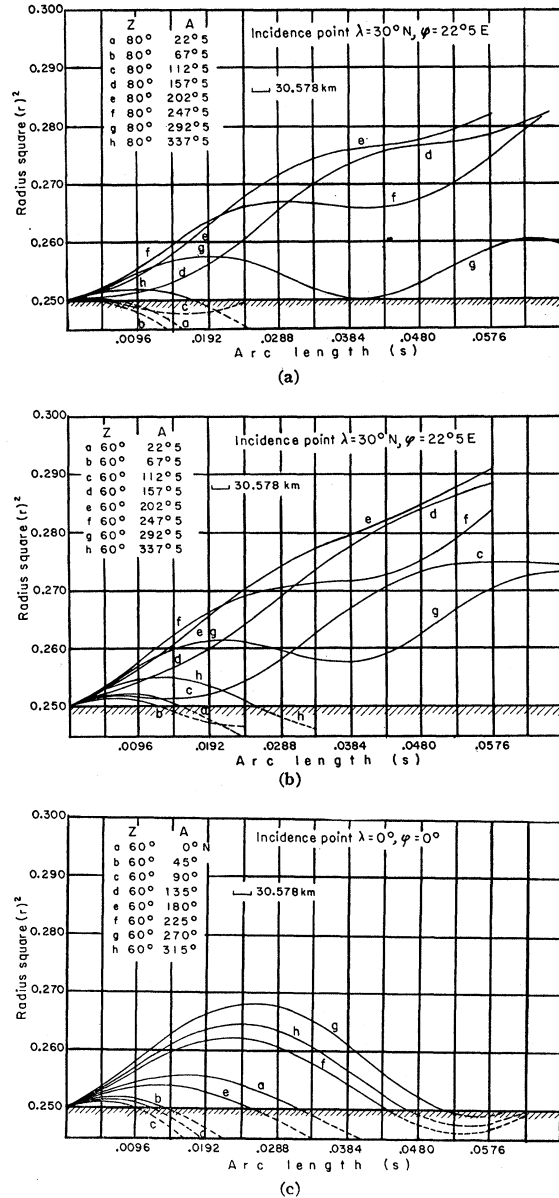


FIG. 6. The effect of the azimuth angle on the albedo. Trajectories of protons of 0.5 Bev. The tables give the values of the azimuth angles of incidence for constant zenith angles. (a) and (b) show trajectories that meet at the same point of incidence but under different zenith angles; (b) and (c) show trajectories that enter with the same zenith angle (60°) but fall on two different points on the earth. The comparison of these two plots illustrates the influence of the latitude on the azimuth effect.

the trajectories on a plane. In some of the figures, the shaded area represents the earth's surface.

DISCUSSION

The object of the present work was to obtain a model of the albedo of cosmic rays. We hope that it will be of use in the experimental work presently carried out in the low-energy region of the spectrum. In the computa-

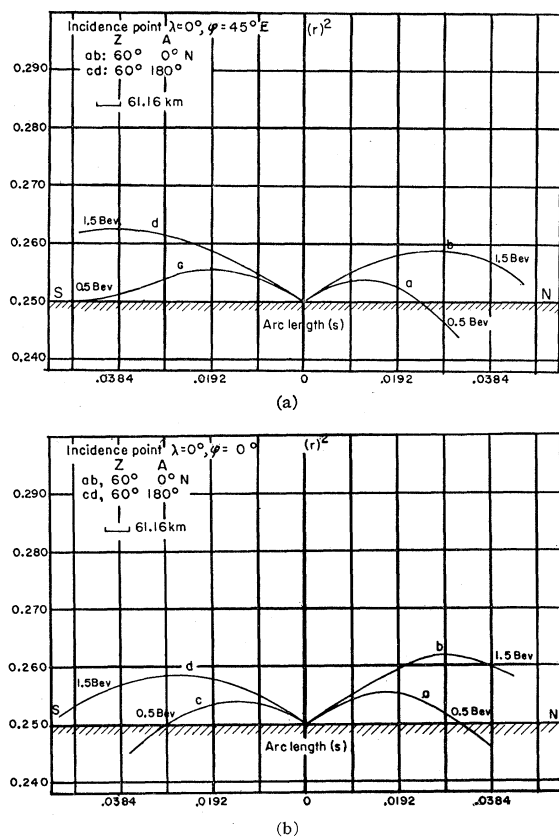


FIG. 7. The asymmetry caused by the magnetic quadrupole. Albedo trajectories incident on the geomagnetic equator. The tables indicate the directions of incidence and the longitudes of the two points of observation. For greater clarity, the northern orbits were drawn to the right and the southern to the left.

tions we have ignored the presence of the atmosphere and its possible interactions with the albedo. The analysis of this model is based on 412 trajectories computed and illustrated in the figures. The maximum length of travel is 860 km, consequently nothing definite can be said about orbits which do not return to the earth within this path length. The trajectories which do return within this limit are said to be in the earth's shadow.

Figures 2 and 6(c) indicate that at the geomagnetic equator, at 0° longitude, all orbits for energies 0.5 BeV or less are in the earth's shadow. On the other hand, for higher energies, the particles approaching from the western directions may come from outside. Only 50% of the orbits of 2-BeV protons are in the earth's shadow. For higher latitudes (see Fig. 3), the percentage of

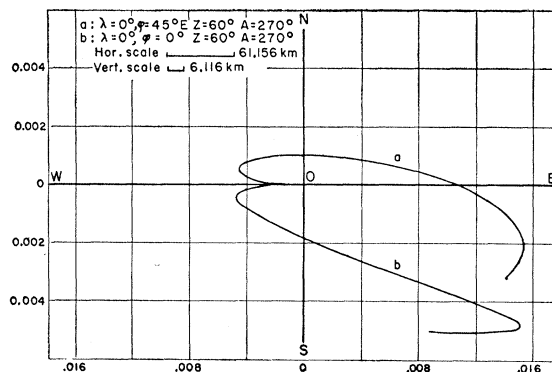


FIG. 8. The effect of the magnetic quadrupole on the albedo trajectories. Projections on local horizontal planes of two protons trajectories of energy 0.5 BeV incident on the equator, in the same local directions. To compare the trajectories, the projection planes were superimposed. The table gives the incidence direction and the longitudes of the observation points.

orbits in the earth's shadow diminishes and is 30% for 0.5 BeV and 25% for 2 BeV protons. The number of orbits in the earth's shadow is smaller in the WSW directions [see Figs. 6(a) and 6(b)]. At latitudes of 60°N and 75°N , only orbits for very small zenith angles were calculated; these do not return to the earth.

A more detailed study of shadow cones and the comparison with those obtained by Schremp would require the calculation of a greater number of orbits.

For greater magnetic rigidity, the particle reaches greater distance from the earth's surface (see Fig. 4).

The zenithal effect on albedo [Figs. 5(a) and 5(b)] seems to indicate that for two latitudes studied (0° , 30°N), the intensity of albedo increases with the increase of the zenith angle.

The quadrupole is most important at the geomagnetic equator, in the vicinity of the earth, for particles of low rigidity. In order to study the quadrupole effect, trajectories of low-energy protons (0.5 and 1.0 BeV) incident on two different points of the geomagnetic equator were considered. At the point of incidence of 0° longitude, the magnetic quadrupole field is horizontal and directed towards the east; at the other point ($\varphi=45^\circ\text{E}$) the quadrupole field is radial. In Figs. 7(a), 7(b), and 8 the asymmetry of albedo, due to the difference in the two local fields, is shown.

ACKNOWLEDGMENTS

The authors wish to express their thanks to Dr. Manuel Sandoval Vallarta by whom this work was suggested and under whose guidance it was carried out.